Animal Nutrition 13 (2023) 249–260

Contents lists available at ScienceDirect

Animal Nutrition

journal homepage: http://www.keaipublishing.com/en/journals/aninu/

Original Research Article

Proteomic and phosphoproteomic analysis reveal threonine deficiency increases hepatic lipid deposition in Pekin ducks via reducing STAT phosphorylation

Yong Jiang [a, c], Zhong Zhuang [a], Wenqia Jia [a], Zhiguo Wen [d, *], Ming Xie [b], Hao Bai [a], Yulin Bi [a], Zhixiu Wang [a], Guobin Chang [a], Shuisheng Hou [b], Guohong Chen [a, *]

[a] College of Animal Science and Technology, Yangzhou University, Yangzhou 225009, China
[b] State Key Laboratory of Animal Nutrition, Key Laboratory of Animal (Poultry) Genetics Breeding and Reproduction, Ministry of Agriculture and Rural Affairs, Institute of Animal Sciences, Chinese Academy of Agricultural Sciences, Beijing 100193, China
[c] Joint International Research Laboratory of Agriculture and Agri-Product Safety, the Ministry of Education of China, Institutes of Agricultural Science and Technology Development, Yangzhou University, Yangzhou 225009, China
[d] Key Laboratory of Feed Biotechnology of Ministry of Agriculture and Rural Affairs, Institute of Feed Research, Chinese Academy of Agricultural Sciences, Beijing 100081, China

ARTICLE INFO

Article history:
Received 16 July 2022
Received in revised form
16 January 2023
Accepted 19 January 2023
Available online 23 January 2023

Keywords:
Threonine deficiency
Triglyceride accumulation
Proteomic
Phosphoproteomic
Pekin duck

ABSTRACT

Dietary threonine (Thr) deficiency enhances triglyceride (TG) deposition in the liver of Pekin ducks, which injures hepatic function and impairs growth performance. However, the underlying molecular mechanisms remain unclear. In the present study, we investigated the effects of dietary Thr deficiency on the expressions of proteins and phosphoproteins in liver of Pekin ducks, to identify the underlying molecular changes. A total of 300 one-day-old ducklings were divided into 3 groups with 10 replicates of 10 birds. All ducks were fed corn-wheat-peanut meal diets containing 0.46%, 0.71%, and 0.96% Thr, respectively, from 1 to 21 days of age. Growth performance, serum parameters, hepatic TG content, and expression of genes involved in lipid metabolism of Pekin ducks were determined. A Thr deficiency group (Thr-D, 0.46% Thr) and a Thr sufficiency group (Thr-S, 0.71% Thr) were selected for subsequent proteomic and phosphoproteomic analysis. The results showed that Thr-D reduced the growth performance ($P < 0.001$), and increased the plasma concentrations of cholesterol, high-density lipoprotein cholesterol, low-density lipoprotein cholesterol, and hepatic TG ($P < 0.05$). Thr-D increased gene expression related to fatty acid and TG synthesis ($P < 0.05$). A total of 176 proteins and 259 phosphosites (containing 198 phosphoproteins) were observed to be differentially expressed as a result of Thr-D. The upregulated proteins were enriched in the pathway related to amino acid metabolism, peroxisome. The downregulated proteins were enriched in linolenic and arachidonic acid metabolism, and the Janus kinase-signal transducer and activator of transcription (JAK-STAT) signaling pathway. The upregulated phosphoproteins were enriched in the pathways related to fatty acid biosynthesis, fructose and mannose metabolism, and glycolysis/gluconeogenesis. Thr-D reduced the phosphorylation of STAT1 at S729 and STAT3 at S728, and expression of STAT5B. In contrast, Thr-D increased non-receptor tyrosine-protein kinase (TYK2) expression and STAT1 phosphorylation at S649. Taken together, dietary Thr-D increased hepatic TG accumulation by upregulating the expression of genes and proteins, and phosphoproteins related to fatty acid and triglyceride synthesis. Furthermore, these processes might be regulated by the JAK-STAT signaling pathway, especially the phosphorylation of STAT1 and STAT3.

* Corresponding authors.
E-mail addresses: wenzhiguo@caas.cn (Z. Wen), ghchen2019@yzu.edu.cn (G. Chen).
Peer review under responsibility of Chinese Association of Animal Science and Veterinary Medicine.

Production and Hosting by Elsevier on behalf of KeAi

https://doi.org/10.1016/j.aninu.2023.01.008

1. Introduction

As a limiting amino acid, threonine (Thr) plays a major role in lots of metabolic processes in humans and poultry (Kidd and Kerr, 1996). The symptoms of experimental animals resulting from dietary Thr deficiency (Thr-D) are anorexia, excessive energy consumption, impaired immunity, and growth inhibition (Jiang et al., 2016; Ross-Inta et al., 2009; Xie et al., 2014; Zhang et al., 2016). Previous studies indicated that dietary Thr-D leads to lipid accumulation in the liver in rats (Methfessel et al., 1964), and also elevates fat concentration of breast muscle and whole body in broilers (Ciftci and Ceylan, 2004; Rangel-Lugo et al., 1994). Recently, we had testified that dietary Thr deficiency elevates triglyceride content in the liver and decreases abdominal fat percentage in ducks (Jiang et al., 2017, 2019a, 2019b, 2020).

Lipid deposition in the liver is a complicated process, and it is unclear how Thr is regulated in the processes. Previous research found that Thr deficiency increases lipid deposition in the liver via reducing lipid catabolism and increasing lipid synthesis pathways (Methfessel et al., 1964). Indeed, we reported that several genes in the liver involved in lipid uptake and fatty acid synthesis are upregulated by dietary Thr-D in Pekin ducks (Jiang et al., 2019a). Furthermore, hepatic transcriptomics analysis revealed that 1,125 genes differentially expressed in Pekin ducks are caused by dietary Thr deficiency, and demonstrated that dietary Thr deficiency upregulates the expression of genes involved in fatty acid and triglyceride synthesis, and downregulates the expression of genes involved in degradation of fatty acids and triglycerides (Jiang et al., 2019b). However, the molecular mechanism underlying post-translational regulation of Thr in hepatic lipid metabolism in Pekin ducks is less well understood both quantitatively and qualitatively.

Proteomics and phosphoproteomic analysis are useful technologies with which to explore the key proteins involved in regulating metabolic pathways influenced by specific nutrients or other dietary factors (Ardito et al., 2017; Wang et al., 2006). Transcriptome and proteome analysis clarified the genes and proteins related to the pathway that increases hepatic lipid deposition in rat induced by zinc deficiency (Dieck et al., 2005). Phosphoproteomic identified phosphorylation sites related to increased lipid metabolism in adipose tissue in dairy cows fed diets with conjugated linoleic acid (Daddam et al., 2021). Thus, proteomics and phosphoproteomic technologies could comprehensively can protein expressions and protein phosphorylation data, which would help to increase understanding of hepatic lipid deposition induced by dietary Thr deficiency.

Therefore, the current study was executed to elucidate the hepatic protein and phosphoprotein expressions in the liver of Pekin ducks fed with Thr deficient diets by applying proteomics and phosphoproteomic technology to elucidate the potential molecular alterations related to hepatic lipid accumulation caused by Thr deficiency.

2. Materials and methods

2.1. Animal ethics statement

The experimental procedures were approved by the Animal Management Committee (in charge of animal welfare issues) of the Institute of Animal Science, Chinese Academy of Agricultural Sciences (IAS 2020-113).

2.2. Animals and experimental design

A total of 300 male Pekin ducks (1 day old) were randomly distributed to 3 treatments (10 replicate cages with 10 ducklings/cage). All the experimental ducks were fed a basal diet (Table 1) or the basal diet with addition of 0.25% and 0.50% Thr from 1 to 21 days of age. The basal diet was prepared to meet the requirements of Pekin ducks according to the National Research Council (NRC, 1994). The experimental birds were housed in cages (200 cm × 100 cm × 40 cm) with wire floors. Feed and water were accessed freely. The dietary Thr concentrations were 0.41% (Thr deficiency, Thr-D), 0.66% (Thr sufficiency, Thr-S), and 0.91% (Thr excess, Thr-E) by calculation.

2.3. Sample collection and preparation

At 21 days of age, the weight of the bird and surplus diet was measured after 12 h fasting to calculate the average body weight of animals in each cage for each treatment. Then 3 ducks were selected from each pen and blood was collected from the jugular vein into a heparinized syringe. The plasma was separated from the blood by centrifuging at 1,000 × *g* for 15 min, and was frozen at −20 °C. The 3 selected ducks were euthanized by CO_2 inhalation. Liver was separated and frozen in liquid nitrogen, and another part of the liver was frozen at −20 °C. The other 4 birds fed with 0.46% Thr and 0.71% Thr were euthanized by CO_2 inhalation and liver samples were collected for phosphoproteomic and proteomics analysis.

2.4. Plasma parameters

Plasma indicators, such as low-density lipoprotein cholesterol (LDLC), triglycerides (TG), high-density lipoprotein cholesterol (HDLC) and total cholesterol, were detected by an automatic analyser (Hitachi 7080, Tokyo, Japan) according to the protocol of a commercial kit (Maccura, Sichuang, China).

2.5. Hepatic triglycerides

The hepatic TG concentrations were detected according to the instructions of commercial kits (Nanjing Jiangcheng Bioengineering institute, NanJing, China).

Table 1
Composition and nutrient levels of the basal diet for Pekin ducks from 1 to 21 days of age (%, as fed basis).

Ingredients	Content	Nutrient levels[1]	Content
Corn	24.8	Metabolizable energy, kcal/kg	2918
Peanut meal	20.0	Crude protein	19.87
Wheat	48.5	Lysine	1.14
Dicalcium phosphate	1.85	Methionine	0.48
Limestone	1.13	Methionine + Cysteine	0.72
Salt	0.30	Tryptophan	0.24
Methionine	0.23	Arginine	1.38
Tryptophan	0.06	Threonine	0.41
Lysine	0.66	Valine	0.76
Valine	0.12	Isoleucine	0.64
Isoleucine	0.11	Calcium	0.90
Corn starch + Thr[2]	0.30	Total phosphorus	0.68
Premix[3]	0.50	Nonphytate phosphorus	0.45
Total	100		

[1] These values are as formulated.
[2] Crystalline threonine supplements added in place of equivalent weights of corn starch.
[3] Supplied per kilogram of total diet: Cu ($CuSO_4 \bullet 5H_2O$), 10 mg; Fe ($FeSO_4 \bullet 7H_2O$), 60 mg; Zn (ZnO), 60 mg; Mn ($MnSO_4 \bullet H_2O$), 80 mg; Se ($NaSeO_3$), 0.3 mg; I (KI), 0.2 mg; choline chloride, 750 mg; vitamin A (retinyl acetate), 8,000 IU; vitamin D_3 (cholecalciferol), 3,000 IU; vitamin E (DL-α-tocopheryl acetate), 20 IU; vitamin K_3 (menadione sodium bisulphate), 2 mg; thiamine (thiamine mononitrate), 1.5 mg; riboflavin, 4 mg; pyridoxine hydrochloride, 3 mg; cobalamin, 0.02 mg; calcium-D-pantothenate, 10 mg; nicotinic acid, 50 mg; folic acid, 1 mg; and biotin, 0.15 mg.

Table 2
Effects of dietary threonine levels on growth performance of ducks from 1 to 21 days of age.

Item	Low	Middle	High	Pooled SEM	*P*-value
Body weight, g	611.89[b]	1,362.99[a]	1,352.67[a]	25.51	<0.001
Weight gain, g/d	26.42[b]	62.20[a]	61.71[a]	1.02	<0.001
Feed intake, g/d	42.53[b]	90.39[a]	90.89[a]	1.62	<0.001
Feed:Gain, g/g	1.61[a]	1.4[b]	1.47[b]	0.03	<0.001

Low = Basal diet without threonine supplementation; Middle = Basal diet supplemented with 0.25% threonine; High = Basal diet supplemented with 0.50% threonine.
[a, b] Mean values with different superscript letters are significantly different ($P < 0.05$).

Table 3
Effects of dietary threonine levels on plasma parameters and hepatic TG of ducks at 21 days of age.

Item	Low	Middle	High	Pooled SEM	*P*-value
Cholesterol, mg/dL	7.22[a]	5.42[b]	5.42[b]	0.22	<0.001
TG, mM	0.37	0.41	0.41	0.014	>0.05
HDLC, mM	3.68[a]	2.80[b]	2.84[b]	0.063	<0.001
LDLC, mM	1.84[a]	1.47[b]	1.37[b]	0.061	<0.001
Hepatic TG, mmol/gprot	7.84[a]	6.36[b]	5.56[b]	0.48	<0.05

Low = Basal diet without threonine supplementation; Middle = Basal diet supplemented with 0.25% threonine; High = Basal diet supplemented with 0.50% threonine; TG = Total triglycerides; HDLC = High-density lipoprotein cholesterol; LDLC = Low-density lipoprotein cholesterol.
[a, b] Mean values with different superscript letters are significantly different ($P < 0.05$).

2.6. RNA isolation and qPCR

RNA isolation, reverse transcription, and quantitative PCR (qPCR) were conducted according to the protocol of commercial kits (Code no. 9109, RR036A, RR820A, TaKaRa, DaLian, China). Briefly, 0.5 mg of total RNA was used to synthesize cDNA according to instructions. The mRNA abundance of target genes was determined by performing qPCR, with β-actin used as a housekeeping gene, and was calculated with the method of $2^{-\triangle\triangle Ct}$ reported by a previous reference (Livak and Schmittgen, 2001). Primers are listed in Table S1.

2.7. Analysis of proteomics and phosphoproteomic in liver

Eight samples (4 biological replicates per group) from the 0.46% Thr and 0.71% Thr groups were used for proteomics and phosphoproteomic analysis according to the description of a previous study(Li et al., 2020). Briefly, the sample was ground into cell powder under liquid nitrogen, and dissolved in lysis buffer with 4 volumes of powder (8 M urea, 1% phosphatase inhibitors, 1% Protease Inhibitor Cocktail). Then the solution was centrifuged at 12,000 × *g* at 4 °C for 10 min, and gathered for further analysis. Then the supernatant was precipitated with cold 20% trichloroacetic acid (TCA) for 2 h at −20 °C, and washed with cold acetone 3 times. The volume of solution was decreased in 5 mM dithiothreitol at 56 °C for 30 min, and alkylated in 11 mM iodoacetamide for 15 min in darkness. The sediment was then diluted with 100 mM TEAB, and added trypsin (1:50 trypsin-to-protein mass ratio) for digestion overnight, and then was digested for 4 h again in 1:100 trypsin-to-protein mass ratio.

The peptide sediment was resuspended in 0.5 M TEAB buffer and labelled using TMT Mass Tag Labeling kits according to the protocol (Thermo Scientifc). The tryptic peptides were fractionated

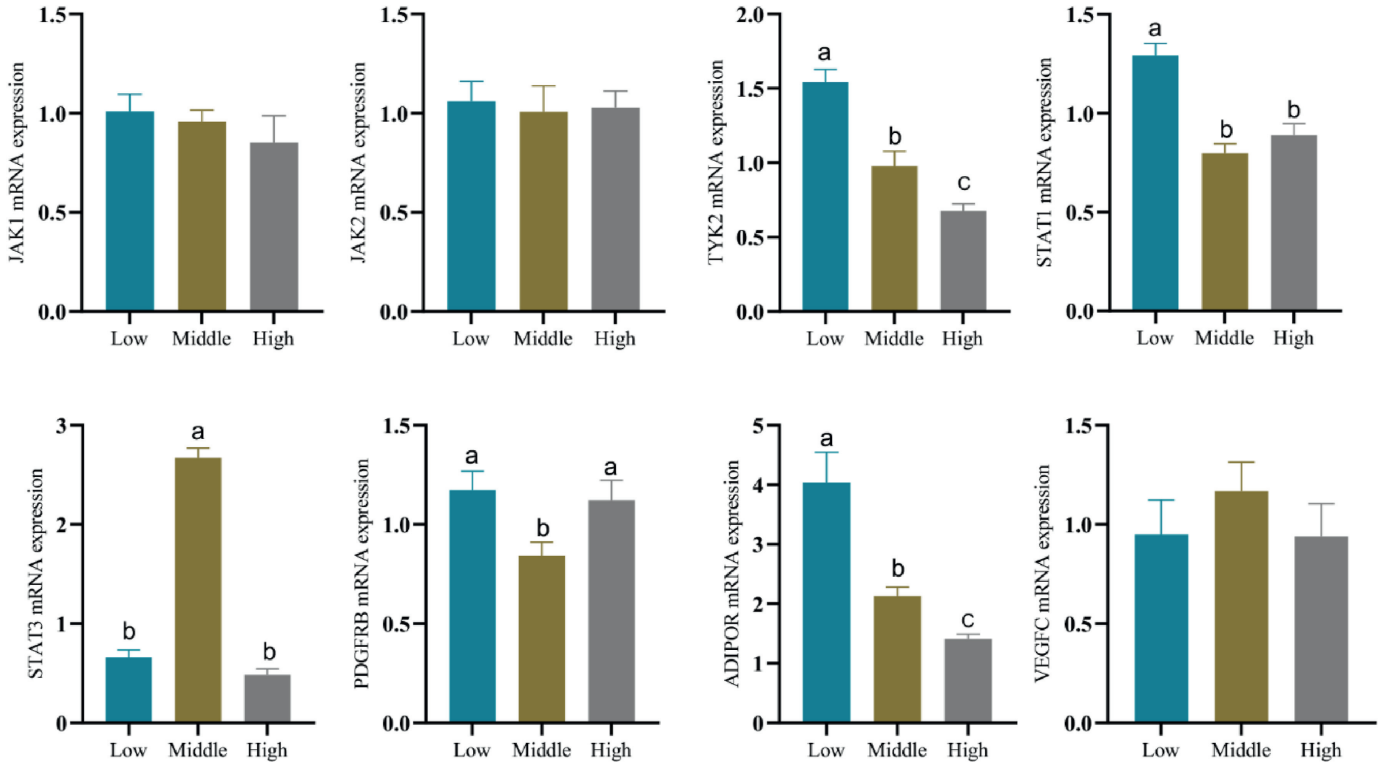

Fig. 1. The effects of dietary threonine levels on gene expression in the Janus kinase-signal transducer and activator of transcription (JAK-STAT) pathway. Bars with different superscript letters are significantly different ($P < 0.05$). *STAT1* = Signal transducer and activator of transcription 1; *STAT3* = Signal transducer and activator of transcription 3; *STAT5B* = Signal transducer and activator of transcription 5B; *PDK2* = Pyruvate dehydrogenase kinase 2; *TYK2* = Non-receptor tyrosine-protein kinase 2; *PDGFRB* = Platelet-derived growth factor receptor beta; *ADIPOR* = Adiponectin receptor; *JAK1* = Janus kinase 1; *JAK2* = Janus kinase 2.

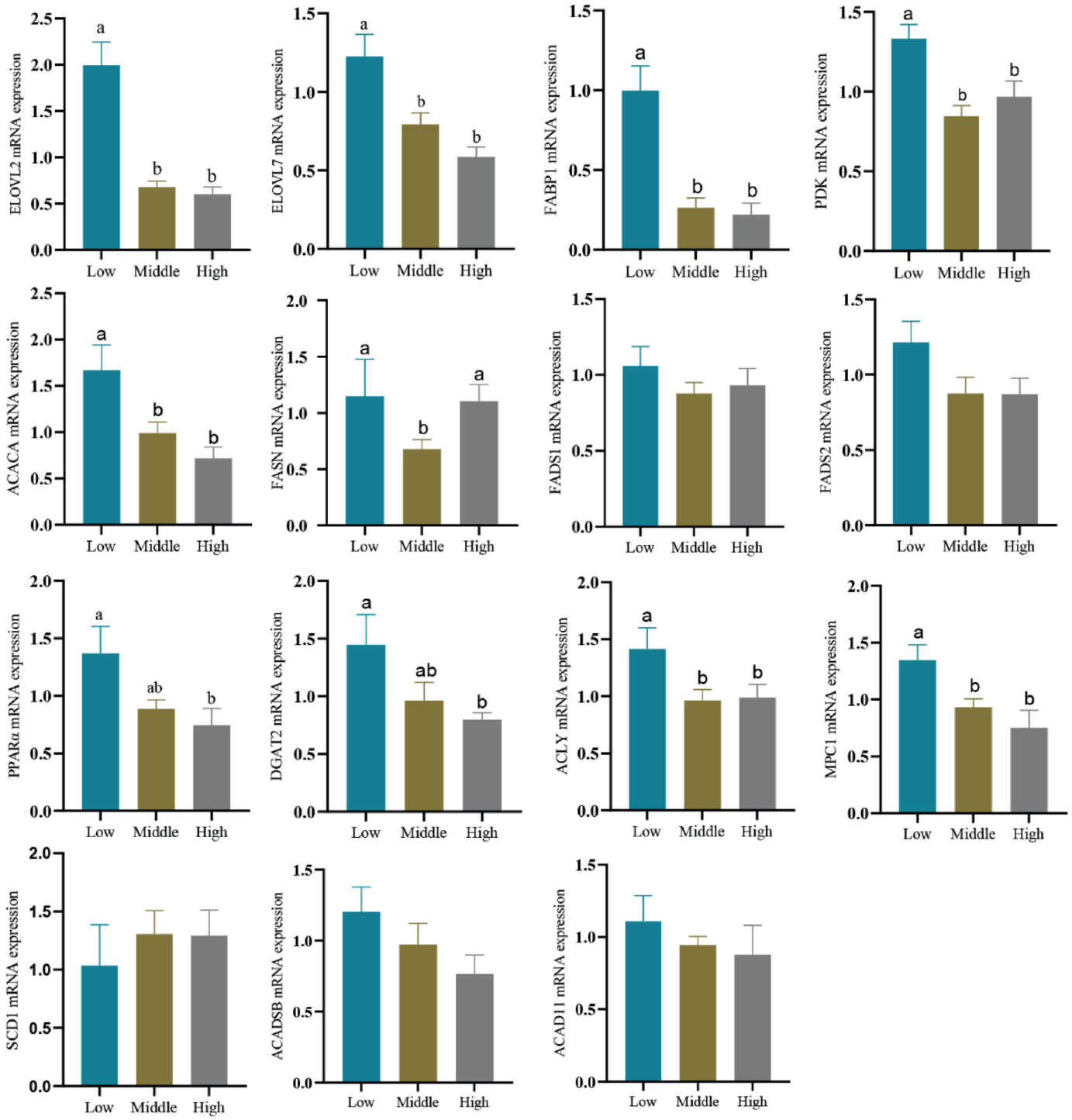

Fig. 2. The effects of dietary threonine levels on the expression of genes involved in lipid metabolism. Bars with different superscript letters are significantly different ($P < 0.05$). *ELOVL2* = Elongation of very long chain fatty acids protein 2; *ELOVL7* = Elongation of very long chain fatty acids protein 7; *PDK2* = Pyruvate dehydrogenase kinase 2; *FABP1* = Fatty acid-binding protein 1; *ACLY* = ATP citrate lyase; *MPC1* = Mitochondrial pyruvate carrier 1; *DGAT2* = Diacylglycerol O-acyltransferase 2; *ACAD11* = Acyl-CoA dehydrogenase family member 11; *ACADSB* = Acyl-CoA dehydrogenase, short/branched chain; *FADS1* = Fatty acid desaturase 1; *FADS2* = Fatty acid desaturase 2; *FASN* = Fatty acid synthase; *PPARα* = Peroxisome proliferator activated receptor α; *SCD* = Stearoyl-CoA desaturase 1; *ACACA* = Acetyl-CoA carboxylase alpha.

with high pH reverse-phase HPLC with a C18 column (Agilent 300 Extend, 5 μm × 4.6 mm × 250 mm). Then, the solutions were mixed into 6 tubes and dried with vacuum centrifuging.

The phosphopeptides were concentrated according to the protocol of IMAC. Briefly, dried peptides were resuspended with IMAC microsphere suspensions, and the microsphere were collected by centrifugation. The IMAC microspheres were washed sequentially (50% ACN/6% TFA and 30% ACN/0.1% TFA). The concentrated phosphopeptides were then collected with elution buffer (10% NH_4OH) and lyophilized, and then dissolved in solvent in 0.1% formic acid containing 2% acetonitrile. The LC-MS/MS analysis was conducted as described in a previous study (Li et al., 2020). The MS/MS spectra

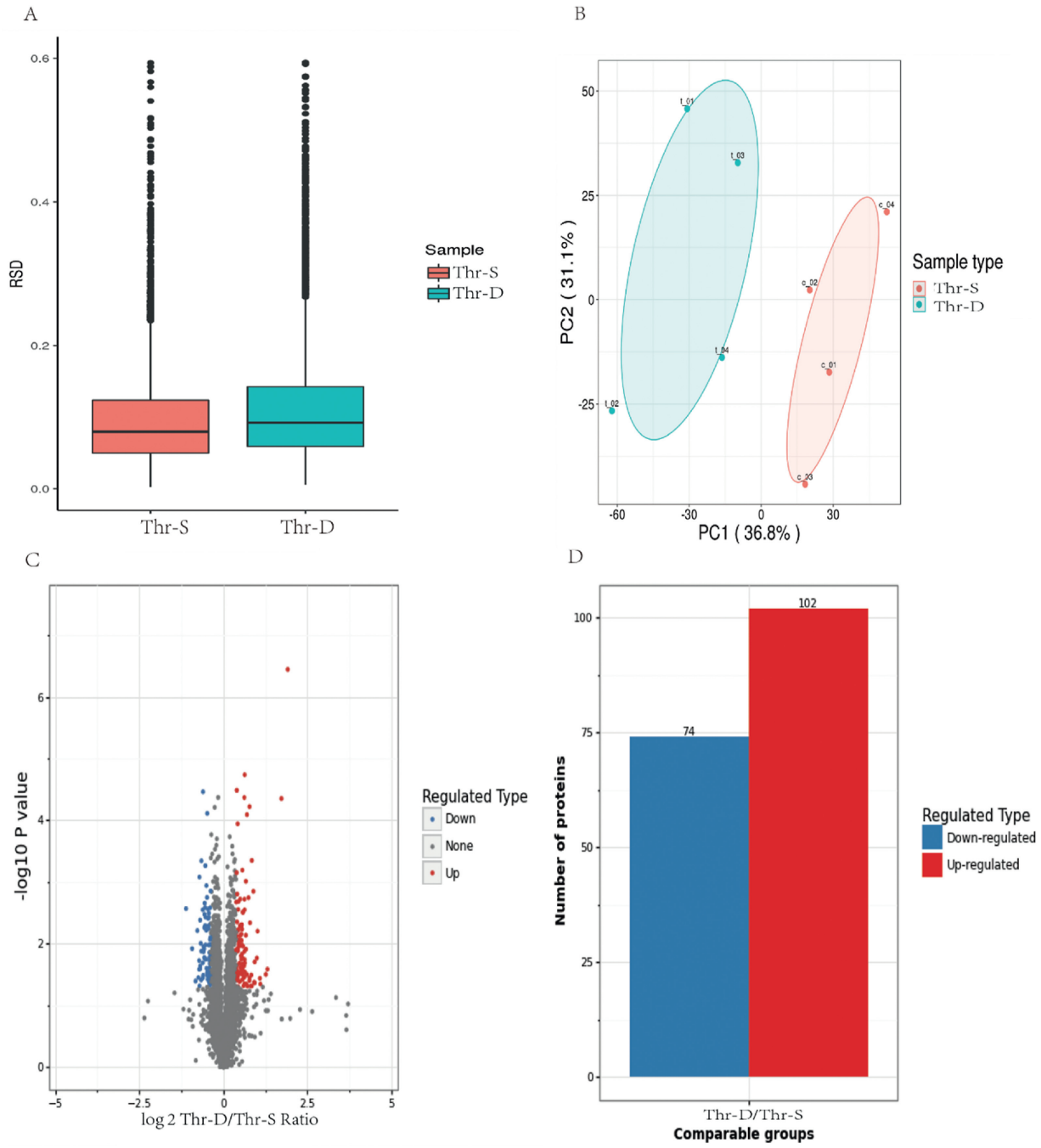

Fig. 3. Proteomic analysis between a threonine deficiency group (Thr-D, 0.46% Thr) and a threonine sufficiency group (Thr-S, 0.71% Thr). (A) Boxplot of quantitative RSD distribution of proteins between repeated samples. (B) The principal component analysis. (C) Volcano map of the differential proteins identified by proteomics analysis. (D) The number of differentially expressed proteins by proteomics analysis.

were searched with Maxquant search engine (v.1.5.2.8). The search and bioinformatic analysis was conducted as per the description of a previous study (Li et al., 2020).

2.8. Statistical analysis

Data was analysed using SAS 9.4 with a general linear model. Statistical significance of means was assessed with Duncan's method. $P < 0.05$ was considered statistically significant.

3. Results

3.1. Growth performance

The dietary Thr level affected the growth performance of ducks (Table 2). Compared to Thr-S, Thr-D reduced the body weight (BW), weight gain (WG), feed intake (FI), and feed to gain ratio (F:G) of Pekin ducks ($P < 0.001$). However, Thr-E level had no influence on BW, WG, FI, and F:G of Pekin ducks ($P > 0.05$).

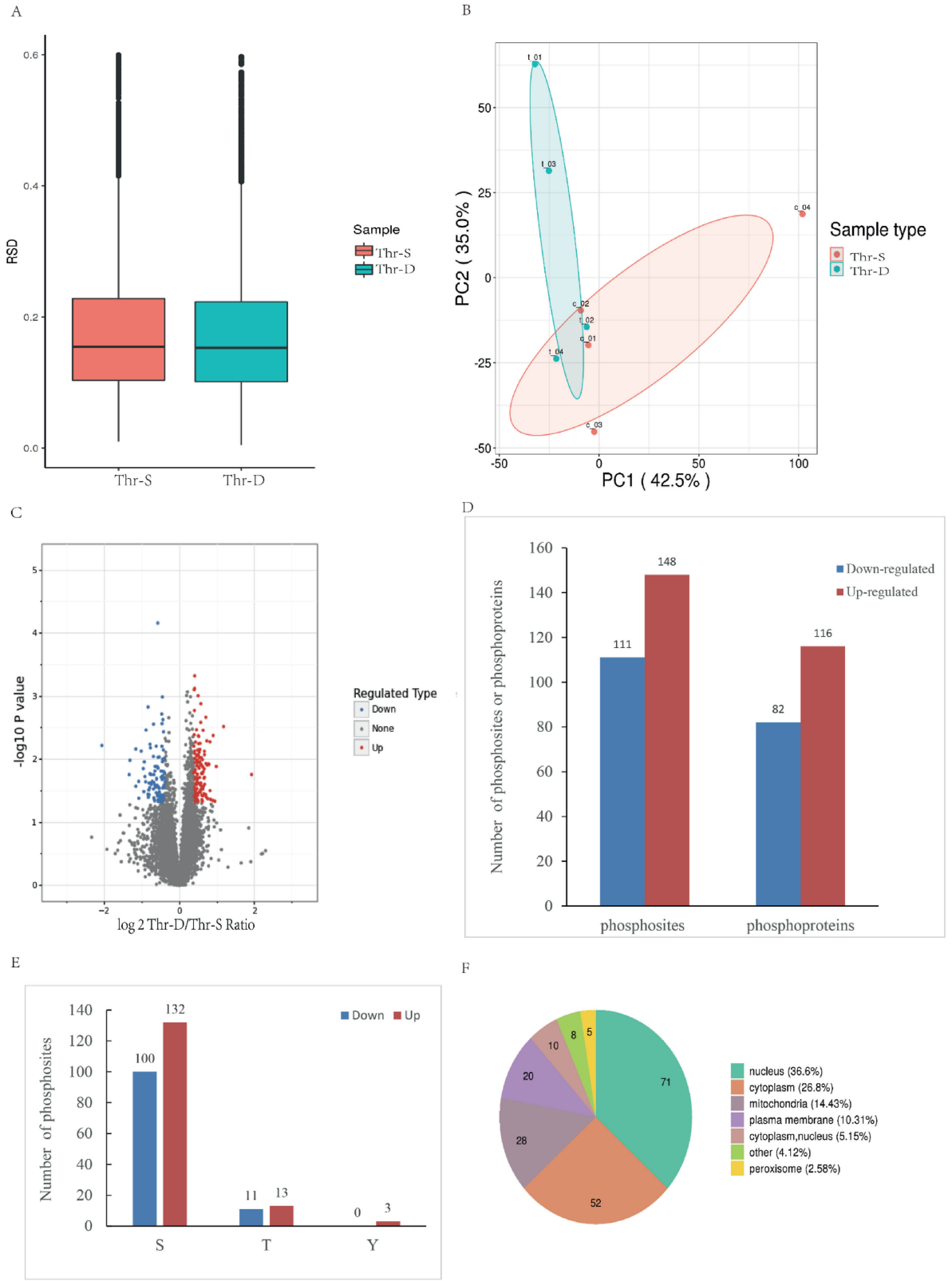

Fig. 4. Phosphoproteomic analysis between a threonine deficiency group (Thr-D, 0.46% Thr) and a threonine sufficiency group (Thr-S, 0.71% Thr). (A) Boxplot of quantitative RSD distribution of phosphosites between repeated samples. (B) The principal component analysis. (C) Volcano map of the differential phosphosites by phosphoproteomic analysis. (D) The number of differential phosphosites and expressed phosphoproteins identified by phosphoproteomic analysis. (E) Distribution of the number of different amino acid modification sites identified. (F) Subcellular localization charts of differentially expressed phosphoproteins.

Motif		Score	Foreground matches	Fold increase	Motif		Score	Foreground matches	Fold increase
	xxxRRx_S_Dxxxxx	38.51	47	21		xxxxxx_T_PPxxxx	32.00	157	24.7
	xxxxxD_S_DxExxx	41.46	101	19		xxxRxx_T_Pxxxxx	28.39	72	22.4
	xxxxxx_S_DDExxx	42.27	76	21.2		xxxxxx_T_PTxxxx	26.97	74	19.9
	xxxxxx_S_DEExxx	48.00	89	16		xxxxxx_T_PExxxx	22.15	66	15.3
	xxxxxx_S_DEDxxx	46.35	65	17.4	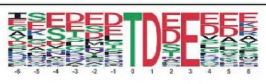	xxxxxx_T_DxExxx	32.00	50	21.1
	xxxxxx_S_DDDxxx	45.49	54	24.1		xxxRRx_T_xxxxxx	28.47	33	18.8
	xxxxxD_S_DxDxxx	38.62	26	18.5					

Fig. 5. Relative position-specific amino acid frequencies around serine/threonine-phosphorylated sites.

3.2. Serum parameters and hepatic lipid

Dietary Thr-D elevated the concentrations of cholesterol, LDLC and HDLC in serum (Table 3, $P < 0.001$) and hepatic TG content. However, Thr-E had no influence on cholesterol, LDLC and HDLC concentrations in serum. Dietary Thr level had no influence on TG concentration in serum.

3.3. Hepatic gene expression

Dietary Thr-D increased the mRNA expression of signal transducer and activator of transcription 1 (*STAT1*) mRNA, non-receptor tyrosine-protein kinase (*TYK2*), platelet-derived growth factor receptor beta (*PDGFRB*), and adiponectin receptor (*ADIPOR*) (Fig. 1, $P < 0.05$), and reduced *STAT3* mRNA expression. Thr-E reduced *STAT3* mRNA expression ($P < 0.05$), and increased *PDGFRB* mRNA expression ($P < 0.05$). Dietary Thr levels had no influence on the mRNA expression of Janus kinase 1 (*JAK1*), *JAK2*, and vascular endothelial growth factor C (*VEGFC*).

Dietary Thr-D increased the mRNA expression of elongation of very long chain fatty acid protein 2 (*ELOVL2*), *ELOVL7*, fatty acid-binding protein 1 (*FABP1*), pyruvate dehydrogenase kinase (*PDK*), acetyl-CoA carboxylase alpha (*ACACA*), fatty acid synthase (*FASN*), peroxisome proliferator activated receptor α (*PPARα*), diacylglycerol O-acyltransferase 2 (*DGAT2*), ATP citrate lyase (*ACLY*), and mitochondrial pyruvate carrier 1 (*MPC1*) (Fig. 2, $P < 0.05$). Thr-E increased *FASN* mRNA expression ($P < 0.05$), and had no influence on mRNA expression of *ELOVL2*, *ELOVL7*, *FABP1*, *PDK*, *ACACA*, *PPARα*, *DGAT2*, *ACLY*, and *MPC1*. Dietary Thr levels did not affect the mRNA expression of fatty acid desaturase 1 (*FADS1*), *FADS2*, stearoyl-CoA desaturase 1 (*SCD1*), acyl-CoA dehydrogenase, short/branched chain (*ACADSB*), and acyl-CoA dehydrogenase family member 11 (*ACAD11*).

3.4. Proteomic and phosphoproteomic analysis

The relative standard deviation (RSD) of media intra-group for proteomics was lower than 0.1 for the 4 biological replicate samples from the Thr-D group and Thr-S group (Fig. 3A), and PCA analysis showed a difference between Thr-D and Thr-S groups (Fig. 3B), indicating high reproducibility of the 4 repeated samples between the two groups. A total of 5,005 proteins were identified in the experiments. A total of 4,754 proteins was quantified, of which 176 were significantly altered (ratio change >1.3 in either direction and *P*-value < 0.05) by Thr-D (Fig. 3C), of which 102 differential expression proteins (DEP) were upregulated, and 74 DEP were downregulated (Fig. 3D).

The media intra-group RSD for phosphoproteomic was similar between the Thr-D and Thr-S groups (Fig. 4A). PCA analysis showed a difference between the Thr-D and Thr-S groups (Fig. 4B). The results indicated high reproducibility of the 4 repeated samples between both groups. Meanwhile, a total of 6,347 quantified sites were identified and 1,896 phosphoproteins were quantified within the eight samples. Moreover, a total of 259 phosphosites showed a significant difference (ratio change >1.3 in either direction and *P*-value < 0.05) between the Thr-D and Thr-S groups (Fig. 4C and D), including 232 phospho-serine (100 downregulated sites, 132 upregulated sites), 24 phosphothreonine (11 downregulated sites, 13 upregulated sites), and 3 upregulated phospho-tyrosine sites (Fig. 4E). A total of 198 phosphoproteins were found to be significantly different (ratio change >1.3 in either direction and *P*-value < 0.05), of which 116 were upregulated and 82 were downregulated (Fig. 4D). More differential expression phosphorylated proteins (DEPP) contained one or two phosphorylation sites, but a small number of proteins were phosphorylated in up to 15 sites. The DEPP were mainly distributed in the nucleus, mitochondria and cytoplasm (Fig. 4F).

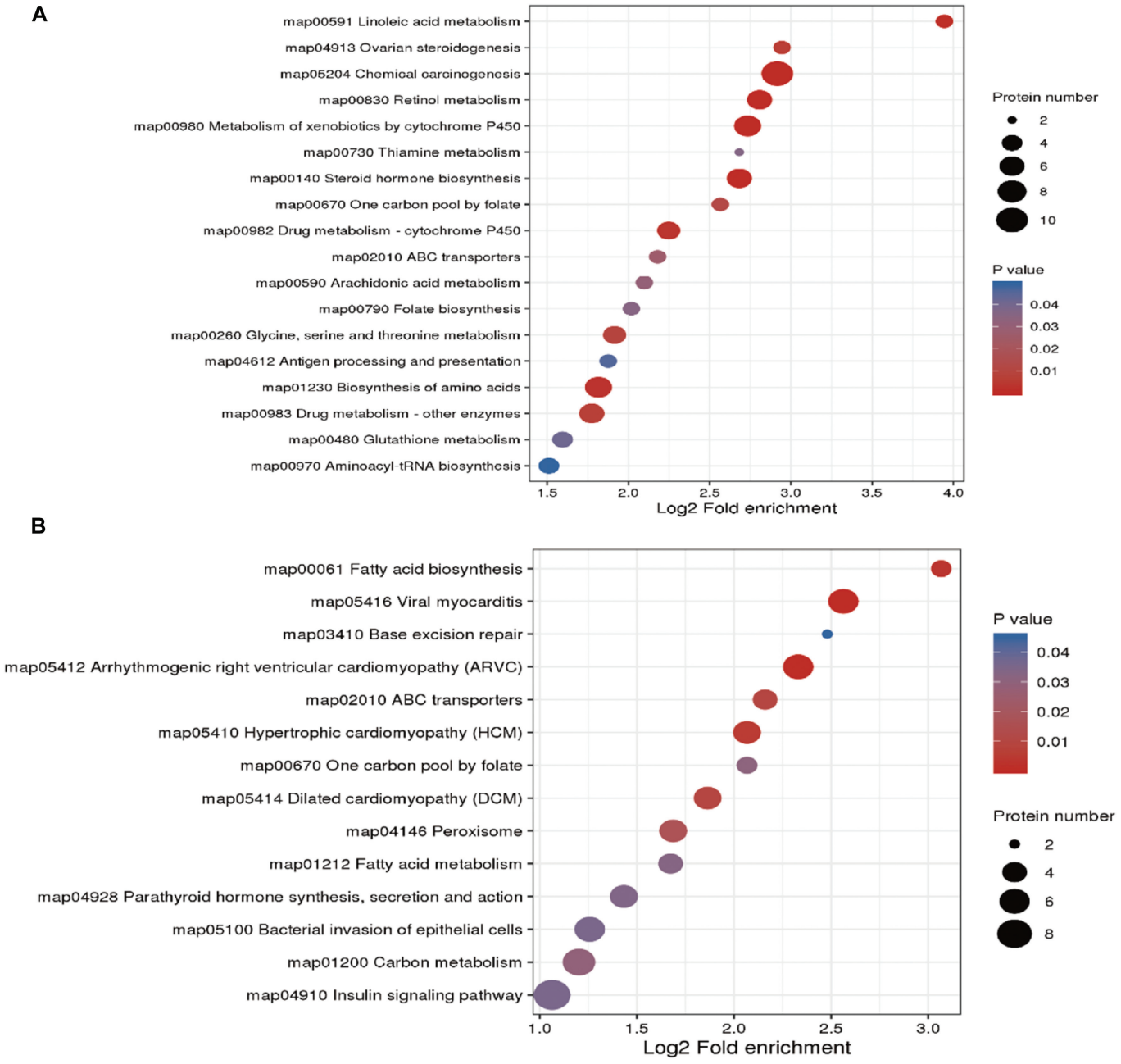

Fig. 6. Analysis of KEGG pathway enrichment of differential expressed proteins (A) and phosphoproteins (B).

3.5. Conserved sequence motif

The phosphosites were subjected to motif-X software for conserved sequence analysis. There were 113 enriched motifs, of which 7 phosphoserine motifs and 6 phosphothreonine motifs were highly enriched motifs (fold increase >15). The motifs of [SD], [TD] and [TP] were frequently occurred in the present study. The number of phosphoserine motifs was higher than that of phosphothreonine motifs. The fold increases in motifs [SDDD] and [TPP] were as high as 24.1 and 24.7, respectively (Fig. 5).

3.6. KEGG analysis

KEGG pathway analysis indicated that all DEP were mainly grouped into 18 functional classes (Fig. 6A), such as "linolenic acid metabolism", "steroid hormone biosynthesis", "ABC transporters", "glycine, serine, and Thr metabolism", "arachidonic acid metabolism", "biosynthesis of amino acids", "Glutathione metabolism" and "aminoacyl-tRNA biosynthesis". All the differentially expressed phosphoproteins were grouped into 14 functional classes (Fig. 6B), such as "fatty acid biosynthesis", "ABC transporter", "peroxisome", "fatty acid metabolism", "parathyroid hormone synthesis, secretion and action" and "insulin signalling pathway". Protein functional analysis showed proteins PDK, uccinyl-CoA:3-ketoacid coenzyme A transferase 1 (OXCT1) and ACLY were downregulated, and MPC1, ELOVL2, FABP1 and TYK2 were upregulated by Thr-D (Table 4).

All the differentially expressed protein and phosphoproteins in the present study were classified into 4 categories (Fig. 7A and B): Q1 ($0 < \text{ratio} < 0.67$), Q2 ($0.67 < \text{ratio} < 0.77$), Q3 ($1.3 < \text{ratio} < 1.5$) and Q4 ($\text{ratio} > 1.5$) according to a previous method (Li et al., 2020).

Table 4
Differentially expressed proteins or phosphoproteins involved in lipid metabolism caused by threonine deficiency in ducks on day 21.

Item	Treat/control ratio	*P*-value	Annotation
Glycolysis			
HK-S479	1.316	< 0.01	Putative hexokinase HKDC1 isoform X2
GAPDH-S23	1.309	< 0.05	Glyceraldehyde-3-phosphate dehydrogenase isoform X2
FBP-Y217	1.395	< 0.05	Fructose-1,6-bisphosphatase
MDH1-S333	1.545	< 0.05	Malate dehydrogenase 1
PDK	0.73	< 0.01	Pyruvate dehydrogenase kinase, isozyme 4
OXCT1	0.749	< 0.05	Uccinyl-coa:3-ketoacid coenzyme A transferase 1
ACLY	0.627	< 0.01	ATP-citrate synthase isoform X1
MPC1	1.309	< 0.05	Mitochondrial pyruvate carrier 1
Lipid metabolism			
FASN-S275	1.566	< 0.05	Fatty acid synthase isoform X1
ACSL-S634	1.482	< 0.05	Long-chain-fatty-acid–coa ligase 5
ELOVL2	2.017	< 0.01	Elongation of very long chain fatty acids protein 2
FABP1	1.621	< 0.05	Fatty acid-binding protein 1
CART-S238	0.735	< 0.05	Carnitine O-acetyltransferase
ACACA-S116	1.340	< 0.05	Acetyl-coa carboxylase 1
AACS	0.584	< 0.01	Acetoacetyl-coa synthetase isoform X1
ACOX2-S650	1.500	< 0.01	Peroxisomal acyl-coenzyme A oxidase 2
ACOX2-S657	1.334	< 0.05	Peroxisomal acyl-coenzyme A oxidase 2
ACOX1	0.621	< 0.01	Peroxisomal acyl-coenzyme A oxidase 1 isoform X2
JAK-STAT signalling pathway			
IRS2-S957	0.678	< 0.05	Insulin receptor substrate 2
TYK2	1.316	< 0.001	Non-receptor tyrosine-protein kinase
STAT1-S649	1.388	0.05	Signal transducer and activator of transcription 1-alpha/beta
STAT1-S729	0.658	< 0.05	Signal transducer and activator of transcription 1-alpha/beta
STAT3-S728	0.716	< 0.05	Signal transducer and activator of transcription 3
STAT5B	0.768	< 0.05	Signal transducer and activator of transcription 5B
PDGFRB	0.763	< 0.01	Platelet-derived growth factor receptor beta
ADIPOR	1.712	< 0.05	Adiponectin receptor protein 2

JAK-STAT = Janus kinase-signal transducer and activator of transcription; HK-S479 = The phosphorylation of putative hexokinase HKDC1 isoform X2 at serine 479 sites; GAPDH-S23 = The phosphorylation of glyceraldehyde-3-phosphate dehydrogenase isoform X2 at serine 23 sites; FBP-Y217 = The phosphorylation of fructose-1,6-bisphosphatase at tyrosine 217 sites; MDH1-S333 = The phosphorylation of malate dehydrogenase 1 at serine 333 sites; FASN-S275 = The phosphorylation of fatty acid synthase isoform X1 at serine 275 sites; ACSL-S634 = The phosphorylation of long-chain-fatty-acid-coa ligase 5 at serine 634 sites; CART-S238 = The phosphorylation of carnitine O-acetyltransferase at serine 238 sites; ACACA-S116 = The phosphorylation of acetyl-coa carboxylase 1 at serine 116 sites; ACOX2-S650 = The phosphorylation of peroxisomal acyl-coenzyme A oxidase 2 at serine 650 sites; ACOX2-S657 = The phosphorylation of peroxisomal acyl-coenzyme A oxidase 2 at serine 657 sites; IRS2-S957 = The phosphorylation of insulin receptor substrate 2 at serine 957 sites; STAT1-S649 = The phosphorylation of signal transducer and activator of transcription 1-alpha/beta at serine 649 sites; STAT1-S6729 = The phosphorylation of signal transducer and activator of transcription 1-alpha/beta at serine 726 sites; STAT3-S728 = The phosphorylation of signal transducer and activator of transcription 3 at serine 729 sites.

Functional analysis of all DEP showed “glycine, serine, and Thr metabolism”, “peroxisome”, “aminoacyl-tRNA biosynthesis”, “biosynthesis of amino acids”, “ABC transporter” and “steroid hormone biosynthesis” were upregulated pathways (Fig. 7C). The cluster “linolenic acid metabolism”, “arachidonic acid metabolism”, “JAK-STAT signaling pathway” and “glutathione metabolism” were downregulated pathways (Fig. 7C). Functional analysis of all quantified phosphoproteins showed “fructose and mannose metabolism”, “fatty acid biosynthesis”, “ABC transporter”, “glycolysis/gluconeogenesis”, “insulin signalling pathway” and “apoptosis-fly” were upregulated pathways (Fig. 7D). The cluster “peroxisome” and “insulin resistance” were downregulated pathways (Fig. 7D). Thr-D increased the phosphorylation of glyceraldehyde-3-phosphate dehydrogenase (GAPDH), putative hexokinase (HK), malate dehydrogenase (MDH1), FASN, long-chain-fatty-acid-CoA ligase 5 (ACSL) and peroxisomal acyl-coenzyme A oxidase 2 (ACOX2), and reduced the phosphorylation of insulin receptor substrate 2 (IRS2), STAT1, and STAT3 (Table 4).

4. Discussion

Thr is a limiting amino acid for animals, and plays a crucial role in lipid deposition. Thr supplementation reduced the epididymal and perirenal fat pad weights in fat mice induced by a high-fat diet (Ma et al., 2020). Recent studies showed that dietary Thr-D increased the TG content in the liver of Pekin ducks (Jiang et al., 2017, 2019a, 2019b, 2020), which was confirmed in the present study. A previous study of transcriptomic analysis indicated that dietary Thr-D increased the gene expressions involved in fatty acid and TG synthesis, and reduced the gene expressions involved in fatty acid oxidation and TG transport (Jiang et al., 2019b), which results in hepatic triglyceride accumulation. In this study, we identified candidate phosphoproteins and proteins that regulate hepatic TG accumulation during dietary Thr deficiency.

In the present study, a total of 198 phosphoproteins and 176 proteins were differentially expressed between the Thr deficiency group and Thr sufficiency group. One hundred and sixteen phosphoproteins and 102 proteins were upregulated, and 82 phosphoproteins and 74 proteins were downregulated by dietary Thr deficiency. These differentially expressed phosphoproteins and proteins were found to affect glycolysis/gluconeogenesis, fatty acid synthesis, and energy metabolism. Phosphoglucomutase (PGM) catalyses the conversion of glucose-1-phosphate (glucose-1-P) to glucose-6-P (Lee et al., 2014). HK catalyses hexose (such as glucose, fructose) phosphorylation to generate hexose-6-phosphate (hexose-6-P) (Magnani et al., 1992), which is the initial step of glycolysis. Glucose-6-P is catalysed to produce fructose-6-P by glucose-6-phosphate isomerase (Mojzikova et al., 2018), and then generate fructose-1,6-P catalysed by phosphofructokinase (Yi et al., 2012). Fructose-Bisphosphatase (FBP) catalyses the hydrolysis of fructose 1,6-bisphosphate to fructose 6-phosphate in the presence of divalent cations (Zarzycki et al., 2007), which is a rate-limiting enzyme in gluconeogenesis. GAPDH is a vital enzyme that catalyses the first step of the glycolysis pathway (Mustafa et al., 2009). The products of glycrol-3-P and acetyl-CoA from glycolysis are the precursor of lipogenesis. MPC1 Mediates the uptake of pyruvate from the

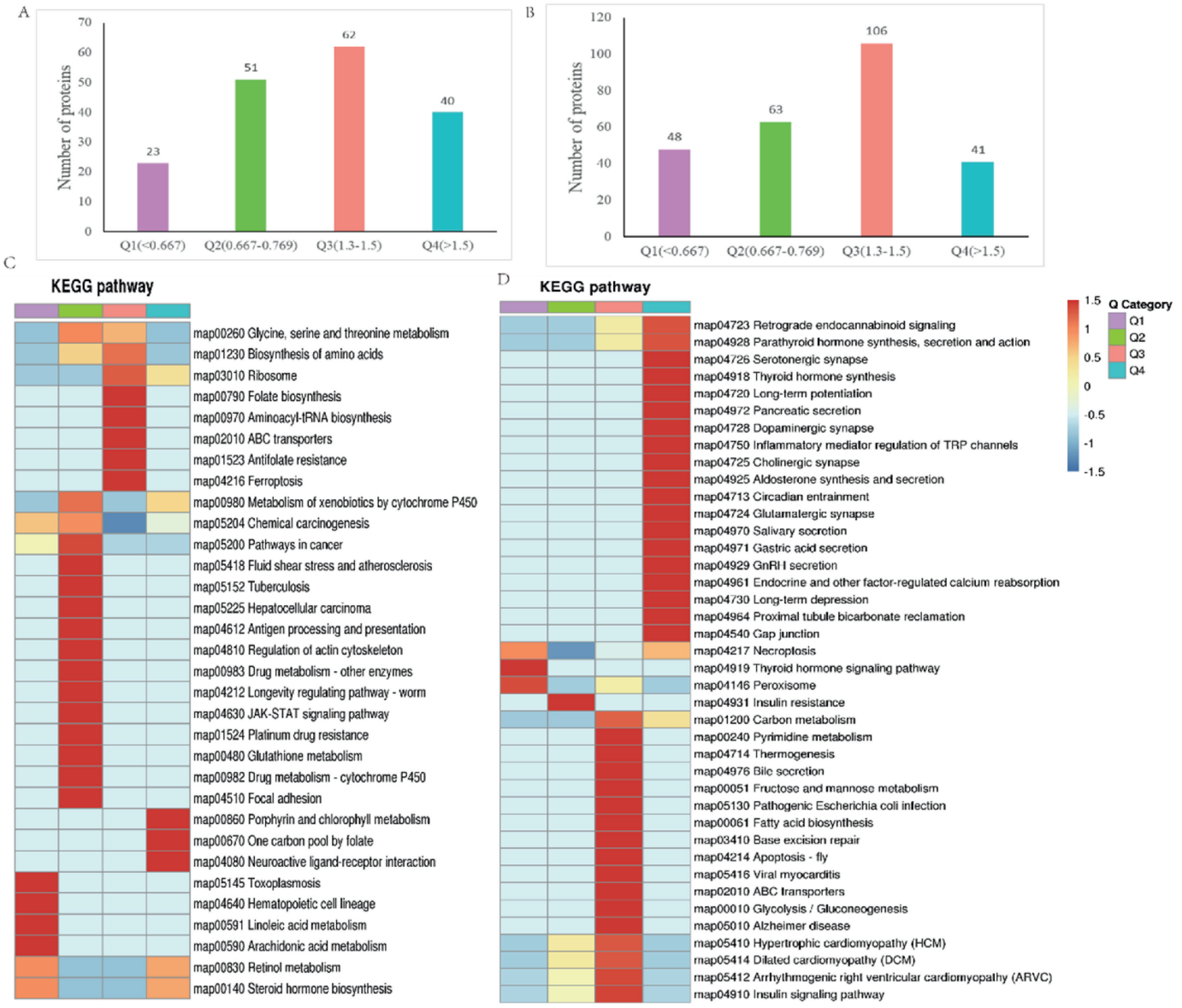

Fig. 7. The distribution histogram of differentially expressed proteins (A) and phosphoproteins (B), KEGG pathway cluster analysis heat map of differentially expressed proteins (C) and phosphoproteins (D) according to the distribution.

cytoplasm into the mitochondria (Le et al., 2021), and then is catalysed to generate Acetyl-CoA by pyruvate dehydrogenase complex (PDHA) (Kato et al., 2008), and thereby links glycolysis to the tricarboxylic cycle. Pyruvate dehydrogenase kinase inhibits the activity of PDHA1 and PDHA2, and thereby regulates metabolite flux through TAC by inhibiting the formation of acetyl-CoA from pyruvate (McFate et al., 2008). In the previous report, dietary Thr deficiency increased the mRNA expression of hexokinase domain containing 1 (*HKDC1*) and enolase 2 (*ENO2*) participating in glycolysis (Jiang et al., 2019b). Dietary methionine deficiency reduced the expression of GAPDH and FBP in the liver of Pekin ducks (Wu et al., 2022). In present experiment, dietary Thr deficiency increased MPC1 expression, and phosphorylation of HK, GAPDH and FBP. However, dietary Thr deficiency reduced PDK protein expression. These results indicated that glycolysis was enhanced and produced more acetyl-CoA for fatty acid synthesis.

The acetyl-CoA produced in mitochondria is transported into the cytoplasm through pyruvate/citrate cycling. Citrate is catalysed to produce oxaloacetate and acetyl-CoA by ACLY (Lin et al., 2013). Oxaloacetate is further catalysed to generate malate by MDH1 (Friedrich et al., 1988). Acetyl-CoA is a substrate for de novo fatty acid synthesis. The phosphorylation of FASN, ACSL, and ACACA were increased by dietary Thr deficiency, and dietary Thr deficiency increased ELOVL2 and FABP1 in the liver. Dietary Thr deficiency also increased the mRNA expression of *ACACA*, *ELOVL2*, *ELOVL7* and *FASN*. ACACA catalyses the carboxylation of acetyl-CoA to malonyl-CoA, which is the first and rate-limiting step in de novo fatty acid synthesis (Hunkeler et al., 2018). FASN is a multifunctional enzyme which catalyses the reaction of acetyl-CoA and malonyl-CoA to produce long-chain saturated fatty acids (Choi et al., 2016). ELOVLs catalyses the synthesis of polyunsaturated very long chain fatty acids from polyunsaturated acyl-CoA and malonyl-CoA (de Antueno et al., 2001). In addition, ACSL catalyses the uptake of fatty acids to produce acyl-CoA to avoid the outflow of fatty acids, and free fatty acids bind to FABPs to form a fatty acid pool to prevent efflux. The acyl-CoAs are used as a substrate for triglyceride

synthesis and oxidation. CRAT catalyses the reversible reaction of acyl groups from carnitine to coenzyme A (CoA), which regulates beta-oxidation (Drecourt et al., 2018). In the current experiment, the proteins and phosphoproteins involved in beta-oxidation and triglyceride synthesis were not found to be differentially expressed, but the *DGAT2* mRNA was upregulated by dietary Thr deficiency, and the mRNA expression of *ACAD11* and *ACADSB* were not changed by dietary Thr deficiency. Previous studies showed that dietary Thr deficiency increased the mRNA expression of *DGAT*, *AGPAT2*, *OXSM*, and *ELOVL7*, and reduced the mRNA expression of *ACAD11* and *ACADSB* (Jiang et al., 2019b). Dietary methionine deficiency also increased FABP1 expression. These results showed that fatty acid synthesis was enhanced by dietary Thr deficiency, and mainly used for triglyceride synthesis, which explains the reasons for increased hepatic TG accumulation induced by Thr deficiency.

Insulin receptor substrate (IRS) plays a crucial role in insulin signal transduction, and thus participates in biological processes regulated by insulin. For example, IRS1 and IRS2 regulate lipid metabolism and blood glucose metabolism (Kido et al., 2000). IRS1 plays a crucial role in hepatic glucose homeostasis, whereas IRS2 takes more of a part in the regulation of hepatic lipid metabolism (Taniguchi et al., 2005). IRS1 knockdown increased the mRNA expression of hepatic nuclear factor 4α, gluconeogenic enzymes and glucose 6-phosphatase as well as phosphoenolpyruvate carboxykinase, whereas knockdown of IRS2 increased hepatic *SREBP1C* mRNA. IRS2 knockout increased the content of glucose, TG, free fatty acids and cholesterol in plasma of C57BL/6J mice compared to wild-type mice, and also increased hepatic lipogenetic enzyme activity, such as ATP citrate lyase, glucose-6-phosphate dehydrogenase, pyruvate kinase and fatty acid synthase (Hashimoto et al., 2006). In the present study, the phosphorylation of IRS2 at Ser 957 was downregulated by dietary Thr deficiency, which would reduce IRS2 activity.

The JAK-STAT signalling pathway participates in lipid metabolism. The STAT family comprises 7 members (1, 2, 3, 4, 5A, 5B and 6) in mammals (Schindler and Darnell, 1995). STATs are predominantly phosphorylated by JAK in tyrosine residue and activated. Tyrosine phosphorylation of STAT leads to the formation of homo- or hetero-dimers, which then translocate into the nucleus to regulate gene expression. STAT1, STAT3, STAT5A and STAT5B play a crucial role in regulating lipid metabolism (Xu et al., 2013). STAT1 inhibits the mRNA expression of peroxisome proliferator-activator receptor γ2 (*PPARγ2*) and lipoprotein lipase (*LPL*). PPARγ2 promotes adipogenesis, while LPL hydrolyzes triglycerides from lipoproteins into free fatty acids in serum, and promotes fatty acid uptake of adipose tissue. STAT1 knockout in mice promotes fatty acid oxidation in adipocytes (Sisler et al., 2015). STAT5A binds to peroxisome proliferator-activator receptor γ (*PPARγ*), while STAT5B binds to C/AAAT enhancer binding protein α (*C/EBPβ*) (Jung et al., 2012), which promotes adipogenesis. The JAK2-STAT3 pathway is related to adipocyte differentiation through regulating C/EBPβ (Zhang et al., 2011). Mice with STAT3 knockout in adipose and liver tissue had higher adipose tissue mass (Cernkovich et al., 2008; Inoue et al., 2004). The phosphorylation of STAT3 promotes lipolysis by upregulating adipose triglyceride lipase (*ATGL*) (Li et al., 2010; Rozovski et al., 2015). Previous studies showed that dietary methionine and choline deficiency regulated hepatic lipid deposition by JAK2 or STAT3 in rats (Kroy et al., 2010; Shi et al., 2017). In addition, methionine improved proliferation and differentiation of intestinal cells in chick embryos via the JAK2-STAT3 signaling pathway (Chen et al., 2021), and promoted crop milk protein synthesis in domestic pigeons by the JAK2-STAT5 signaling pathway (Chen et al., 2020). In the present study, dietary Thr-D decreased the phosphorylation of STAT3 at Ser 728 and STAT1 at Ser 729, and downregulated the expression of STAT5B and upregulated the expression of TYK2, and increased the mRNA expression of *TYK2* and *STAT1*, and reduced *STAT3*. These findings show that Thr might regulate hepatic lipid deposition in ducks though the JAK-STAT pathway.

5. Conclusion

In the current study, dietary Thr-D repressed the growth performance and increased hepatic lipid deposition in ducks. Dietary Thr-D affected the expression of genes, proteins and phosphoproteins. The upregulated genes, proteins and phosphoproteins were related to glycolysis, fatty acid and triglyceride synthesis, which could explain the accumulation of hepatic lipids, which might be regulated by the JAK-STAT signalling pathway. These findings may provide an insightful understanding of the genes, proteins and phosphorylation acting as major regulators of the hepatic lipid deposition process, and it may therefore be useful to help elucidate the molecular mechanisms by which Thr deficiency accelerates hepatic lipid deposition.

Author contributions

Shuisheng Hou conceived and coordinated the study. **Yong Jiang** performed the study and was involved in all aspects of analysis and drafted the manuscript. **Ming Xie** and **Shuisheng Hou** were involved in experimental design. **Ming Xie, Zhixiu Wang, Yulin Bi** and **Hao Bai** performed data analysis. **Zhong Zhuang** and **Wenqia Jia** performed sample analysis. **Zhiguo Wen**, **Guobin Chang** and **Guohong Chen** participated in editing the manuscript. **Zhiguo Wen**, and **Guohong Chen**: had primary responsibility for the final content. All authors read and approved the final version of the manuscript.

Declaration of competing interest

We declare that we have no financial and personal relationships with other people or organizations that might inappropriately influence our work, and there is no professional or other personal interest of any nature or kind in any product, service and/or company that could be construed as influencing the content of this paper.

Acknowledgements

This work was supported by National Natural Science Foundation of China (31902174), Natural Science Foundation of Jiangsu Province (BK20190902), Tackled key technologies in agriculture and rural areas of Jiangsu Science and Technology Plan (BE2022310).

Appendix Supplementary data

Supplementary data to this article can be found online at https://doi.org/10.1016/j.aninu.2023.01.008.

References

Ardito F, Giuliani M, Perrone D, Troiano G, Lo Muzio L. The crucial role of protein phosphorylation in cell signaling and its use as targeted therapy. Int J Mol Med 2017;40:271–80. https://doi.org/10.3892/ijmm.2017.3036.

Cernkovich ER, Deng J, Bond MC, Combs TP, Harp JB. Adipose-specific disruption of signal transducer and activator of transcription 3 increases body weight and adiposity. Endocrinology 2008;149:1581–90. https://doi.org/10.1210/en.2007-1148.

Chen M, Zhou J, Chen Y, Wang X, Yan H, Gao C. The in ovo injection of methionine improves intestinal cell proliferation and differentiation in chick embryos by

activating the JAK2/STAT3 signaling pathway. Anim Nutr 2021;7:1031–8. https://doi.org/10.1016/j.aninu.2021.03.009.
Chen Mg, Pan Nx, Wang Xq, Yan Hc, Gao Cq. Methionine promotes crop milk protein synthesis through the JAK2-STAT5 signaling during lactation of domestic pigeons (Columba livia). Food Funct 2020;11:10786–98. https://doi.org/10.1039/d0fo02257h.
Choi MS, Jung J-Y, Kim H-J, Ham MR, Lee TR, Shin DW. S-nitrosylation of fatty acid synthase regulates its activity through dimerization. J Lipid Res 2016;57:607–15. https://doi.org/10.1194/jlr.m065805.
Ciftci I, Ceylan N. Effects of dietary threonine and crude protein on growth performance, carcase and meat composition of broiler chickens. Br Poult Sci 2004;45:280–9. https://doi.org/10.1080/00071660410001715894.
Daddam JR, Hammon HM, Troescher A, Vogel L, Gnott M, Kra G, et al. Phosphoproteomic analysis of subcutaneous and omental adipose tissue reveals increased lipid turnover in dairy cows supplemented with conjugated linoleic acid. Int J Mol Sci 2021;22:3227. https://doi.org/10.3390/ijms22063227.
de Antueno RJ, Knickle LC, Smith H, Elliot ML, Allen SJ, Nwaka S, et al. Activity of human Delta5 and Delta6 desaturases on multiple n-3 and n-6 polyunsaturated fatty acids. FEBS Lett 2001;509:77–80. https://doi.org/10.1016/s0014-5793(01)03135-0.
Dieck HT, Doring F, Fuchs D, Roth HP, Daniel H. Transcriptome and proteome analysis identifies the pathways that increase hepatic lipid accumulation in zinc-deficient rats. J Nutr 2005;135:199–205. https://doi.org/10.1093/jn/135.2.199.
Drecourt A, Babdor J, Dussiot M, Petit F, Goudin N, Garfa-Traoré M, et al. Impaired transferrin receptor palmitoylation and recycling in neurodegeneration with brain iron accumulation. Am J Hum Genet 2018;102:266–77. https://doi.org/10.1016/j.ajhg.2018.01.003.
Friedrich CA, Ferrell RE, Siciliano MJ, Kitto GB. Biochemical and genetic identity of alpha-keto acid reductase and cytoplasmic malate dehydrogenase from human erythrocytes. Ann Hum Genet 1988;52:25–37. https://doi.org/10.1111/j.1469-1809.1988.tb01075.x.
Hashimoto H, Arai T, Takeguchi A, Hioki K, Kosaka K. Ontogenetic characteristics of enzyme activities and plasma metabolites in C57BL/6J:Jcl mice deficient in insulin receptor substrate 2. Comparative Med 2006;56:176–87.
Hunkeler M, Hagmann A, Stuttfeld E, Chami M, Guri Y, Stahlberg H, et al. Structural basis for regulation of human acetyl-CoA carboxylase. Nature 2018;558:470–4. https://doi.org/10.1038/s41586-018-0201-4.
Inoue H, Ogawa W, Ozaki M, Haga S, Matsumoto M, Furukawa K, et al. Role of STAT-3 in regulation of hepatic gluconeogenic genes and carbohydrate metabolism in vivo. Nat Med 2004;10:168–74. https://doi.org/10.1038/nm980.
Jiang Y, Uzma M, Tang T, Wen ZG, Hou SS, Huang W, et al. Effects of dietary protein on threonine requirements of Pekin ducks from hatch to 21 days of age. Anim Feed Sci Technol 2016;217:95–9. https://doi.org/10.1016/j.anifeedsci.2016.04.010.
Jiang Y, Tang J, Xie M, Wen ZG, Qiao SY, Hou SS. Threonine supplementation reduces dietary protein and improves lipid metabolism in Pekin ducks. Br Poult Sci 2017;58:687–93. https://doi.org/10.1080/00071668.2017.1363871.
Jiang Y, Liao XD, Xie M, Tang J, Qiao SY, Wen ZG, et al. Dietary threonine supplementation improves hepatic lipid metabolism of Pekin ducks. Anim Prod Sci 2019a;59:673–80. https://doi.org/10.1071/an17633.
Jiang Y, Xie M, Fan W, Xue J, Zhou Z, Tang J, et al. Transcriptome analysis reveals differential expression of genes regulating hepatic triglyceride metabolism in pekin ducks during dietary threonine deficiency. Front Genet 2019b;10:710. https://doi.org/10.3389/fgene.2019.00710.
Jiang Y, Xie M, Tang J, Zhou Z, Zhang Y, Chen G, et al. Effects of genetic selection and threonine on meat quality in Pekin ducks. Poult Sci 2020;99:2508–18. https://doi.org/10.1016/j.psj.2019.10.059.
Jung HS, Lee YJ, Kim YH, Paik S, Kim JW, Lee JW. Peroxisome proliferator-activated receptor gamma/signal transducers and activators of transcription 5A pathway plays a key factor in adipogenesis of human bone marrow-derived stromal cells and 3T3-L1 preadipocytes. Stem Cells & Dev 2012;21:465–75. https://doi.org/10.1089/scd.2010.0591.
Kato M, Wynn RM, Chuang JL, Tso S-C, Machius M, Li J, et al. Structural basis for inactivation of the human pyruvate dehydrogenase complex by phosphorylation: role of disordered phosphorylation loops. Structure 2008;16:1849–59. https://doi.org/10.1016/j.str.2008.10.010.
Kidd MT, Kerr BJ. L-threonine for poultry: a review. J Appl Poult Res 1996;5:358–67. https://doi.org/10.1093/japr/5.4.358.
Kido Y, Burks DJ, Withers D, Bruning JC, Accili D. Tissue-specific insulin resistance in mice with mutations in the insulin receptor, IRS-1, and IRS-2. J Clin Invest 2000;105:199–205. https://doi.org/10.1172/JCI7917.
Kroy DC, Beraza N, Tschaharganeh DF, Sander LE, Erschfeld S, Giebeler A, et al. Lack of interleukin-6/glycoprotein 130/signal transducers and activators of transcription-3 signaling in hepatocytes predisposes to liver steatosis and injury in mice. Hepatology 2010;51:463–73. https://doi.org/10.1002/hep.23322.
Le X, Lee C, Millar A. The mitochondrial pyruvate carrier (MPC) complex mediates one of three pyruvate-supplying pathways that sustain Arabidopsis respiratory metabolism. Plant Cell 2021. https://doi.org/10.1093/plcell/koab148.
Lee Y, Stiers KM, Kain BN, Beamer LJ. Compromised catalysis and potential folding defects in in vitro studies of missense mutants associated with hereditary phosphoglucomutase 1 deficiency. J Biol Chem 2014;289:32010–9. https://doi.org/10.1074/jbc.m114.597914.
Li L, Deng M, Lyu C, Zhang J, Peng J, Cai C, et al. Quantitative phosphoproteomics analysis reveals that protein modification and sugar metabolism contribute to sprouting in potato after BR treatment. Food Chem 2020;325:126875. https://doi.org/10.1016/j.foodchem.2020.126875.
Li YC, Zheng XL, Liu BT, Yang GS. Regulation of ATGL expression mediated by leptin in vitro in porcine adipocyte lipolysis. Mol Cell Biochem 2010;333:121–8. https://doi.org/10.1007/s11010-009-0212-4.
Lin R, Tao R, Gao X, Li T, Zhou X, Guan K-L, et al. Acetylation stabilizes ATP-citrate lyase to promote lipid biosynthesis and tumor growth. Mol Cell 2013;51:506–18. https://doi.org/10.1016/j.molcel.2013.07.002.
Livak KJ, Schmittgen TD. Analysis of relative gene expression data using real-time quantitative PCR and the 2(-Delta Delta C(T)) Method. Methods 2001;25:402–8. https://doi.org/10.1006/meth.2001.1262.
Ma Q, Zhou X, Sun Y, Hu L, Shan A. Threonine, but not lysine and methionine, reduces fat accumulation by regulating lipid metabolism in obese mice. J Agric Food Chem 2020;68:4876–83. https://doi.org/10.1021/acs.jafc.0c01023.
Magnani M, Bianchi M, Casabianca A, Stocchi V, Daniele A, Altruda F, et al. A recombinant human 'mini'-hexokinase is catalytically active and regulated by hexose 6-phosphates. Biochem J 1992;285:193–9. https://doi.org/10.1042/bj2850193.
McFate T, Mohyeldin A, Lu H, Thakar J, Henriques J, Halim ND, et al. Pyruvate dehydrogenase complex activity controls metabolic and malignant phenotype in cancer cells. J Biol Chem 2008;283:22700–8. https://doi.org/10.1074/jbc.m801765200.
Methfessel AH, Mudambi S, Harper AE, Falcone AB. Biochemical changes in fatty liver induced by choline or threonine deficiency. ii. various hepatic enzymic activities during the development of fatty livers in rats. Arch Biochem Biophys 1964;104:360–8. https://doi.org/10.1016/0003-9861(64)90475-8.
Mojzikova R, Koralkova P, Holub D, Saxova Z, Pospisilova D, Prochazkova D, et al. Two novel mutations (p.(Ser160Pro) and p.(Arg472Cys)) causing glucose-6-phosphate isomerase deficiency are associated with erythroid dysplasia and inappropriately suppressed hepcidin. Blood Cell Mol Dis 2018;69:23–9. https://doi.org/10.1016/j.bcmd.2017.04.003.
Mustafa AK, Gadalla MM, Sen N, Kim S, Mu W, Gazi SK, et al. H2S signals through protein S-sulfhydration. Sci Signal 2009;2:ra72. https://doi.org/10.1126/scisignal.2000464.
NRC. Nutrient requirements of poultry. 9th rev. ed. Washington, DC: Natl. Acad. Press; 1994.
Rangel-Lugo M, Su CL, Austic RE. Threonine requirement and threonine imbalance in broiler chickens. Poult Sci 1994;73:670–81. https://doi.org/10.3382/ps.0730670.
Ross-Inta CM, Zhang YF, Almendares A, Giulivi C. Threonine-deficient diets induced changes in hepatic bioenergetics. Am J Physiol Gastrointest Liver Physiol 2009;296:G1130–9. https://doi.org/10.1152/ajpgi.90545.2008.
Rozovski U, Grgurevic S, Bueso-Ramos C, Harris D, Li P, Liu Z, et al. Aberrant LPL expression, driven by stat3, mediates free fatty acid metabolism in cll cells. Mol Cancer Res 2015;13:944–53. https://doi.org/10.1158/1541-7786.Mcr-14-0412.
Schindler C, Darnell Jr JE. Transcriptional responses to polypeptide ligands: the JAK-STAT pathway. Annu Rev Biochem 1995;64:621–51. https://doi.org/10.1146/annurev.bi.64.070195.003201.
Shi SY, Luk CT, Schroer SA, Kim MJ, Dodington DW, Sivasubramaniyam T, et al. Janus kinase 2 (jak2) dissociates hepatosteatosis from hepatocellular carcinoma in mice. J Biol Chem 2017;292:3789–99. https://doi.org/10.1074/jbc.M116.752519.
Sisler J, Morgan M, Raje V, Grande R, Derecka M, Meier J, et al. The signal transducer and activator of transcription 1 (stat1) inhibits mitochondrial biogenesis in liver and fatty acid oxidation in adipocytes. PLoS One 2015;10:e0144444. https://doi.org/10.1371/journal.pone.0144444.
Taniguchi CM, Ueki K, Kahn CR. Complementary roles of IRS-1 and IRS-2 in the hepatic regulation of metabolism. J Clin Invest 2005;115:718–27. https://doi.org/10.1172/JCI23187.
Wang J, Li D, Dangott LJ, Wu G. Proteomics and its role in nutrition research. J Nutr 2006;136:1759–62. https://doi.org/10.1093/jn/136.7.1759.
Wu Y, Tang J, Wen Z, Zhang B, Cao J, Zhao L, et al. Dietary methionine deficiency stunts growth and increases fat deposition via suppression of fatty acids transportation and hepatic catabolism in Pekin ducks. J Anim Sci Biotechnol 2022;13:61. https://doi.org/10.1186/s40104-022-00709-z. 61.
Xie M, Zhang L, Wen ZG, Tang J, Huang W, Hou SS. Threonine requirement of White Pekin ducks from hatch to 21 d of age. Br Poult Sci 2014;55:553–7. https://doi.org/10.1080/00071668.2014.929638.
Xu D, Yin C, Wang S, Xiao Y. JAK-STAT in lipid metabolism of adipocytes. JAK-STAT 2013;2:e27203. https://doi.org/10.4161/jkst.27203.
Yi W, Clark PM, Mason DE, Keenan MC, Hill C, Goddard WA, et al. Phosphofructokinase 1 glycosylation regulates cell growth and metabolism. Science 2012;337:975–80. https://doi.org/10.1126/science.1222278.
Zarzycki M, Maciaszczyk E, Dzugaj A. Glu 69 is essential for the high sensitivity of muscle fructose-1,6-bisphosphatase inhibition by calcium ions. FEBS Lett 2007;581:1347–50. https://doi.org/10.1016/j.febslet.2007.02.051.
Zhang K, Guo W, Yang Y, Wu J. JAK2/STAT3 pathway is involved in the early stage of adipogenesis through regulating C/EBP beta transcription. J Cell Biochem 2011;112:488–97. https://doi.org/10.1002/jcb.22936.
Zhang Q, Zeng QF, Cotter P, Applegate TJ. Dietary threonine response of Pekin ducks from hatch to 14 d of age based on performance, serology, and intestinal mucin secretion. Poult Sci 2016;95:1348–55. https://doi.org/10.3382/ps/pew032.